

Stability Analysis of a sea bass and young sea bass model

Masahiro Yamaguchi (山口正博, f0130180@ipc.shizuoka.ac.jp)
 Yasuhiro Takeuchi (竹内康博, takeuchi@sys.eng.shizuoka.ac.jp)

Department of Systems Engineering, Faculty of Engineering,
 Shizuoka University (静岡大学工学部システム工学科)

1 Introduction

In this paper we consider population dynamics of sea bass and young sea bass. It is known that young sea bass eats resource such as a prawn or benthos and when it grows up into sea bass, sea bass eats not only resource but also prey like small fish.

Let $x(t)$ denote the density of resource, $y(t)$ the density of prey and $z(t)$ the density of sea bass at time t . It is assumed that young sea bass and sea bass are divided by age τ . Also, we can neglect predation rate upon resource and reproduction rate of young sea bass since it seems to have little ability of predation and can not reproduce for itself. Based on the above assumptions, we have the model

$$\begin{aligned} x'(t) &= x(t)(r_1 - a_{11}x(t) - a_{12}y(t) - a_{13}z(t)), \\ y'(t) &= y(t)(-r_2 + a_{21}x(t) - a_{23}z(t)), \\ z'(t) &= -r_3z(t) + e^{-l\tau}(a_{31}x(t - \tau) + a_{32}y(t - \tau))z(t - \tau) \end{aligned} \tag{1}$$

with initial conditions

$$\begin{aligned} x(\theta) &= \psi_1(\theta), & -\tau \leq \theta \leq 0, \\ y(\theta) &= \psi_2(\theta), & -\tau \leq \theta \leq 0, \\ z(\theta) &= \psi_3(\theta), & -\tau \leq \theta \leq 0, \end{aligned}$$

where $\psi_i (i = 1, 2, 3)$ are nonnegative continuous functions on $\theta \in [-\tau, 0]$. r_1 is the intrinsic growth rate of resource. r_2 is the death rate of prey. l is the death rate of young sea bass and r_3 is the death rate of sea bass. a_{11} is the density-dependent coefficient of resource. a_{12} and a_{13} are the predation rate of prey and sea bass feeding upon resource respectively. a_{23} is the predation rate of sea bass feeding upon prey. a_{21}/a_{12} is the transformation rate of prey due to predation on resource. a_{31}/a_{13} and a_{32}/a_{23} are the transformation rate of sea bass due to predation on resource and prey respectively. The term

$$e^{-l\tau}(a_{31}x(t - \tau) + a_{32}y(t - \tau))z(t - \tau)$$

represents the number of young sea bass that was born at time $t - \tau$ which still survives at time t and is transferred from the immature stage to the mature stage at time t .

This paper consists of five sections. In Section 2 we consider model (1) without time delay, that is, without young sea bass. The model becomes intra-guild predation model. As a result, we find relatively high predation rate and small transformation rate of sea bass feeding on resource can cause the emergence of chaos. In Section 3 we find existence conditions of the equilibria and some

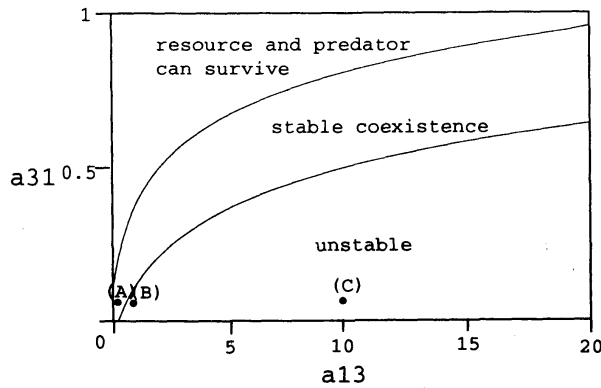


Figure 1: Stability and instability domains for model (2). $r_1 = 5, r_2 = 1, r_3 = 1.2, a_{11} = 0.4, a_{12} = 1, a_{21} = 1, a_{23} = 1, a_{32} = 1$. The values (a_{13}, a_{31}) at (A), (B) and (C) are $(0.1, 0.1)$, $(1.0, 0.1)$ and $(10.0, 0.1)$ respectively.

of their local stability conditions. But it is not easy to find local stability conditions of a positive equilibrium and boundary equilibrium composed of resource and sea bass. With respect to the positive equilibrium, the numerical simulation indicates stability changes from instability to stability as time delay increases. In Section 4, in order to investigate in detail the result obtained in Section 3, we try to apply the geometric stability switch criteria established by Beretta and Kuang [1] to the model. Then, we can obtain a critical value at which the stability switch occurs. Finally, in Section 5 we give future problems.

2 Intra-guild predation ($\tau = 0$)

First of all we consider model (1) with $\tau = 0$, that is, without young sea bass. Then, model (1) becomes the following:

$$\begin{aligned} x'(t) &= x(t)(r_1 - a_{11}x(t) - a_{12}y(t) - a_{13}z(t)), \\ y'(t) &= y(t)(-r_2 + a_{21}x(t) - a_{23}z(t)), \\ z'(t) &= z(t)(-r_3 + a_{31}x(t) + a_{32}y(t)). \end{aligned} \quad (2)$$

Model (2) is called an "intra-guild predation model". Intra-guild predation means a subset of omnivory, which is defined as feeding on resources at different trophic levels. In this model both sea bass and prey feed on the same resource. Holt and Polis [3] showed relatively small amounts of intra-guild predation can strongly destabilize the system. However, whether chaos occurs or not has not been investigated yet. By using numerical simulation, we can obtain trajectory which seems to be chaotic. In the following we show the emergence of chaos numerically.

We fix parameters except a_{13} and a_{31} . Then, as a result of local stability analysis of (2), we can obtain stability and instability domains of equilibria (see Fig.1). Let us choose three points (A), (B) and (C) from Fig.1 so that a_{31} remains constant and a_{13} increases. The value (a_{13}, a_{31}) of each point are respectively $(0.1, 0.1)$, $(1.0, 0.1)$ and $(10.0, 0.1)$. Three figures (a), (b) and (c) in Fig.2 show solution behaviours at (A), (B) and (C) in Fig.1 respectively. These figures indicate as a_{13} increases the solution behaviour changes from stable to periodic and finally becomes chaotic. From a biological point of view, relatively high predation rate and small transformation rate of sea bass feeding on the resource can cause the emergence of chaos.

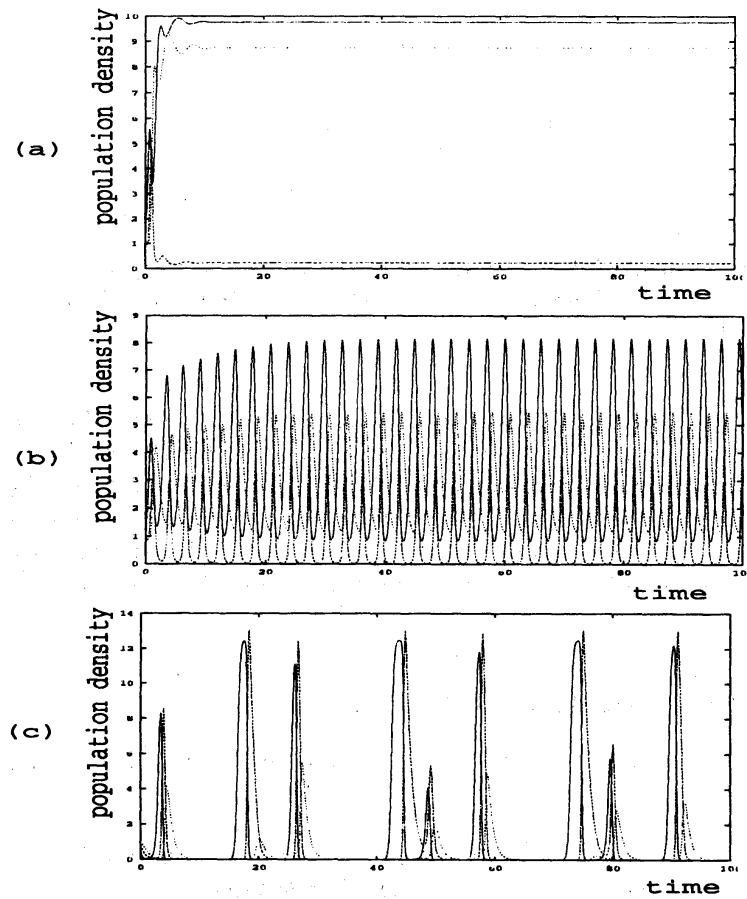


Figure 2: Figures (a), (b) and (c) are solution behaviours at (A), (B) and (C) in Fig.1 respectively. We can see as a_{13} increases the system is destabilized. As a_{13} increases further chaos occurs.

3 Sea bass and young sea bass model ($\tau \neq 0$)

In this section we consider population dynamics of model (1). In Section 3.1 we show existence conditions and some of local stability conditions of the equilibria. However, we can not obtain local stability conditions of a positive equilibrium and boundary equilibrium composed of resource and sea bass. So, in Section 3.2, we investigate local dynamics around the positive equilibrium by using numerical simulation. It shows as time delay τ increases solution behaviour which is unstable at $\tau = 0$ changes to be stable.

3.1 Equilibrium and local stability

Model (1) has five equilibria. Existence conditions and local stability conditions of equilibria are the following table:

equilibrium	existence condition	local stability condition
$E_0 = (0, 0, 0)$	always	unstable
$E_1 = (\frac{r_1}{a_{11}}, 0, 0)$	always	E_2, E_3 do not exist
$E_2 = (\tilde{x}, \tilde{y}, 0)$	$r_1 > r_2 \frac{a_{11}}{a_{21}}$	$\tilde{z} < 0$
$E_3 = (\hat{x}, 0, \hat{z})$	$r_1 > r_3 \frac{a_{11}}{a_{31}} e^{l\tau}$??
$E_4 = \frac{1}{ A }(\tilde{x}, \tilde{y}, \tilde{z})$	$\frac{\tilde{x}}{ A }, \frac{\tilde{y}}{ A }, \frac{\tilde{z}}{ A } > 0$??

where $|A|$ is the determinant of matrix

$$A = \begin{pmatrix} a_{11} & a_{12} & a_{13} \\ -a_{21} & 0 & a_{23} \\ -a_{31} & -a_{32} & 0 \end{pmatrix}.$$

However, it is not so easy to find local stability conditions of E_3 and E_4 . In this paper we try to investigate numerically local dynamics around E_4 .

3.2 Simulation

We consider local dynamics around E_4 . By using the parameters at which solution behaviour is chaotic in model (2), we investigate how the system's behaviour changes as τ increases. Fig.3 (a), (b) and (c) are depicted at respectively $\tau = 0.5, 1.2$ and 1.5 . These figures show as τ increases the solution behaviour which is chaotic at $\tau = 0$ (Fig.2 (c)) changes to periodic one and finally becomes stable one. That is, the increase of time delay τ can stabilize the system. Also, we can observe the stability change from instability to stability at τ between 1.2 and 1.5. However, numerical simulation can not indicate explicitly a critical value at which stability changes. So in the next section, by using geometric stability switch criteria, we will try to find the critical value.

4 Stability switch

4.1 Geometric stability switch criteria

In this section we summarize the theory given by Beretta and Kuang [1]. Let us consider the characteristic equation of model (1)

$$\lambda^3 + a(\tau)\lambda^2 + b(\tau)\lambda + c(\tau) + (d(\tau)\lambda^2 + e(\tau)\lambda + f(\tau))e^{-\lambda\tau} = 0; \quad (3)$$

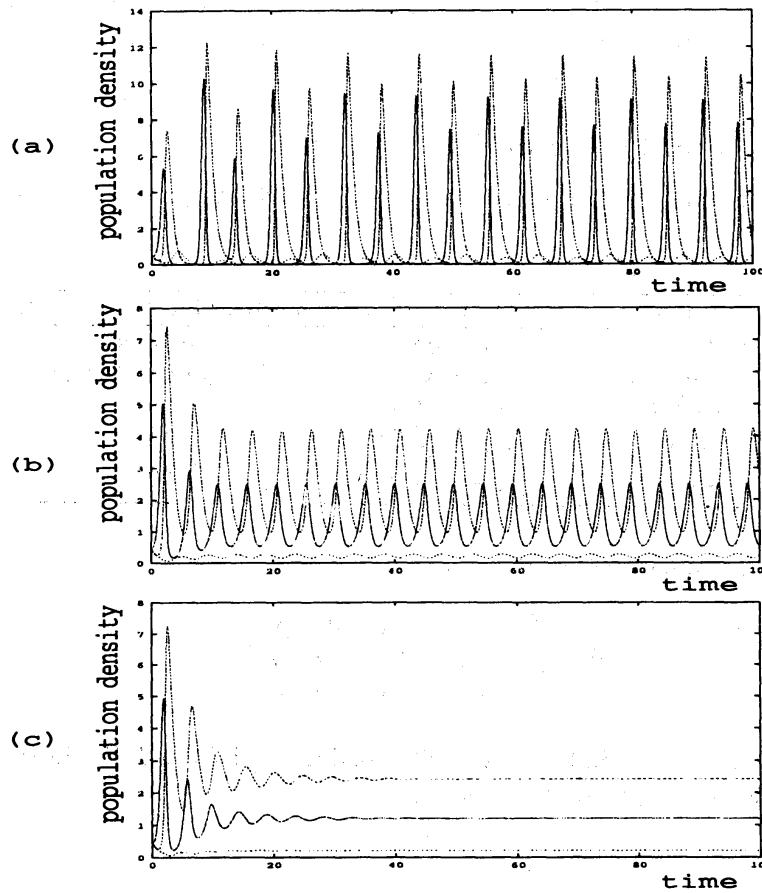


Figure 3: Figures (a), (b) and (c) are depicted at respectively $\tau = 0.5, 1.2$ and 1.5 . Parameters are $r_1 = 5, r_2 = 1, r_3 = 1.2, a_{11} = 0.4, a_{12} = 1, a_{13} = 10, a_{21} = 1, a_{23} = 1, a_{31} = 0.1, a_{32} = 1$. These figures show as time delay τ increases each amplitude of the solution gets smaller. Finally, solution behaviour which is chaotic at $\tau = 0$ (Fig.2 (c)) becomes stable at some value τ between 1.2 and 1.5.

$\tau \in \mathbf{R}_{0+}$ and $a(\tau), b(\tau), c(\tau), d(\tau), e(\tau), f(\tau): \mathbf{R}_{+0} \rightarrow \mathbf{R}$ are differentiable functions of class $C^1(\mathbf{R}_{+0})$ such that $c(\tau) + f(\tau) \neq 0$ for all $\tau \in \mathbf{R}_{+0}$ and for any τ , $d(\tau), e(\tau), f(\tau)$ are not simultaneously zero. We define

$$P(\lambda, \tau) := \lambda^3 + a(\tau)\lambda^2 + b(\tau)\lambda + c(\tau), Q(\lambda, \tau) := d(\tau)\lambda^2 + e(\tau)\lambda + f(\tau).$$

Due to $c(\tau) + f(\tau) \neq 0$, $\lambda = 0$ can not be a root of (3). So a stability switch (or a crossing of the eigenvalue on the imaginary axis) necessarily occurs with $\lambda = \pm i\omega$ with $\omega > 0$. Without loss of generality we assume $\lambda = i\omega, \omega > 0$, as a root of (3). Then $P(\lambda, \tau)$ and $Q(\lambda, \tau)$ are

$$\begin{aligned} P(i\omega, \tau) &= -i\omega^3 - a(\tau)\omega^2 + ib(\tau)\omega + c(\tau), \\ Q(i\omega, \tau) &= -d(\tau)\omega^2 + ie(\tau)\omega + f(\tau). \end{aligned}$$

Now we replace that $P(i\omega, \tau) = P_R(i\omega, \tau) + iP_I(i\omega, \tau)$ and $Q(i\omega, \tau) = Q_R(i\omega, \tau) + iQ_I(i\omega, \tau)$ where

$$\begin{aligned} P_R(i\omega, \tau) &= -a(\tau)\omega^2 + c(\tau), \\ P_I(i\omega, \tau) &= -\omega^3 + b(\tau)\omega, \\ Q_R(i\omega, \tau) &= -d(\tau)\omega^2 + f(\tau), \\ Q_I(i\omega, \tau) &= e(\tau)\omega. \end{aligned}$$

We put $\lambda = i\omega$ into (3), then we have

$$\begin{aligned} \cos \omega\tau &= -\frac{P_R Q_R + P_I Q_I}{|Q(i\omega, \tau)|^2}, \\ \sin \omega\tau &= -\frac{P_R Q_I - P_I Q_R}{|Q(i\omega, \tau)|^2}. \end{aligned} \quad (4)$$

Now we can define $F(\omega)$ as follows and consider

$$F(\omega) \equiv |P(i\omega)|^2 - |Q(i\omega)|^2 = 0. \quad (5)$$

And we can define the angle $\theta \in [0, 2\pi]$, as the solution of (4)

$$\begin{aligned} \cos \theta(\tau) &= -\frac{P_R Q_R + P_I Q_I}{|Q(i\omega, \tau)|^2}, \\ \sin \theta(\tau) &= -\frac{P_R Q_I - P_I Q_R}{|Q(i\omega, \tau)|^2}, \end{aligned} \quad (6)$$

and the relation between the argument θ in (6) and $\omega\tau$ in (4) for $\tau > 0$ must be

$$\omega\tau = \theta + 2n\pi, n \in N_0 := \{0, 1, 2, \dots\}. \quad (7)$$

Hence we can define the maps $\tau_n : I \rightarrow \mathbf{R}_{+0}$ given by

$$\tau_n(\tau) := \frac{\theta(\tau) + 2n\pi}{\omega(\tau)}, \tau_n > 0, n \in N_0 \quad (8)$$

where a positive root $\omega(\tau)$ of (5) exists in I . Let us introduce the functions $I \rightarrow \mathbf{R}$,

$$S_n(\tau) := \tau - \tau_n(\tau) \quad (9)$$

that are continuous and differentiable in τ .

Theorem 4.1 ([1]) Assume that $\omega(\tau)$ is a positive root of (5) defined for $\tau \in I, I \subseteq \mathbf{R}_{+0}$, and at some $\tau^* \in I$

$$S_n(\tau^*) = 0 \text{ for some } n \in \mathbf{N}_0. \quad (10)$$

Then a pair of simple conjugate pure imaginary roots $\lambda = \pm i\omega$ exists at $\tau = \tau^*$ which crosses the imaginary axis from left to right if $\delta(\tau^*) > 0$ and crosses the imaginary axis from right to left if $\delta(\tau^*) < 0$, where

$$\delta(\tau^*) = \text{sign}\{F'_\omega(\omega(\tau^*), \tau^*)\} \text{sign} \left\{ \left. \frac{dS_n(\tau)}{d\tau} \right|_{\tau=\tau^*} \right\}. \quad (11)$$

Remark 4.1 Assume that $\theta(\tau) \in (0, 2\pi), \tau \in I$, where $\theta(\tau)$ is defined by (6). Then we have

$$\begin{aligned} \theta(\tau) &= \arctan(-\eta(\tau)/\phi(\tau)) \text{ if } \sin \theta > 0, \cos \theta > 0; \\ \theta(\tau) &= \pi/2 \text{ if } \sin \theta = 1, \cos \theta = 0; \\ \theta(\tau) &= \pi + \arctan(-\eta(\tau)/\phi(\tau)) \text{ if } \cos \theta < 0; \\ \theta(\tau) &= 3\pi/2 \text{ if } \sin \theta = -1, \cos \theta = 0; \\ \theta(\tau) &= 2\pi + \arctan(-\eta(\tau)/\phi(\tau)) \text{ if } \sin \theta < 0, \cos \theta > 0. \end{aligned}$$

where $\phi(\tau) = P_R Q_R + P_I Q_I$ and $\eta(\tau) = -P_R Q_I + P_I Q_R$.

4.2 Local stability of a positive equilibrium

Let us consider local stability of positive equilibrium E_4 . As we showed in Section 3.1, it is not easy to find rigorously local stability condition of E_4 . So in Section 3.2 we showed the numerical simulation which indicates as time delay increases solution behaviour changes from chaotic to periodic, and finally to stable. In this section, we try to apply Theorem 4.1 and Remark 4.1 to the model in order to obtain a critical value at which stability changes from unstable to stable.

The characteristic equation at $E_4 = (x^*, y^*, z^*)$ takes the form (3) with

$$\begin{aligned} a(\tau) &= a_{11}x^* + r_3, \\ b(\tau) &= a_{12}a_{21}x^*y^* + a_{11}r_3x^*, \\ c(\tau) &= r_3a_{12}a_{21}x^*y^*, \\ d(\tau) &= -e^{-l\tau}(a_{31}x^* + a_{32}y^*), \\ e(\tau) &= e^{-l\tau}(a_{13}a_{31}x^*z^* + a_{23}a_{32}y^*z^* - a_{11}x^*(a_{31}x^* + a_{32}y^*)), \\ f(\tau) &= e^{-l\tau}((a_{11}a_{23}a_{32} + a_{13}a_{21}a_{32} - a_{12}a_{23}a_{31})x^*y^*z^* \\ &\quad - a_{12}a_{21}x^*y^*(a_{31}x^* + a_{32}y^*)). \end{aligned}$$

Fig.4 indicates for $n = 0$

$$\left. \frac{dS_n(\tau)}{d\tau} \right|_{\tau=\tau^*} > 0.$$

Also with respect to F'_ω in Theorem 4.1 we checked numerically it is negative. Then since $\delta(\tau^*)$ in Theorem 4.1 is negative, a pair of imaginary roots moves from the right half plane to the left half plane at critical value $\tau^* = 1.29967$. Further it is easy to check that the Jacobian matrix evaluated at E_4 for $\tau = 0$ with parameter values given in Fig.2 (c) has one negative real and a pair of complex eigenvalues with a positive real part. That is, as we predicted in Section 3.2, at τ^* between 1.2 and 1.5 a stability switch occurs from instability to stability. So we find the increase of time delay has a stabilizing effect for the system. Actually, Fig.3 (b) and (c) show when $\tau < \tau^*$ the solution behaviour is unstable, whereas when $\tau > \tau^*$ it is stable.

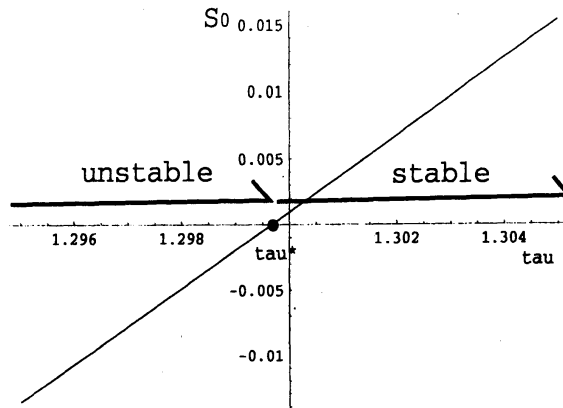


Figure 4: Graph of stability switch in terms of time delay. At $\tau^* = 1.29967$ a pair of imaginary roots moves from the right half plane to the left half plane. Actually, stability changes from instability to stability at τ^* .

5 Discussion

It will be published in another paper by using an average Liapunov function (see [2]) that system (2) is permanent if there exists a positive equilibrium and $|A| > 0$. That is, for three trajectories given in Fig.2, there exist positive constant vectors δ and M such that

$$\delta \leq \liminf_{t \rightarrow +\infty} (x(t), y(t), z(t)) \leq \limsup_{t \rightarrow +\infty} (x(t), y(t), z(t)) \leq M.$$

The interesting future problem is to obtain the corresponding permanence condition for system (1). Some mathematics given in [4] seems to be applicable to our system.

References

- [1] Beretta, E. and Y. Kuang (2002): Geometric Stability Switch Criteria in Delay Differential Systems with Delay Dependent Parameters, *SIAM J. Math. Anal.* Vol. 33, No.5, pp. 1144-1165.
- [2] Hofbauer, J. and K. Sigmund (1998): *Evolutionary Games and Population Dynamics*, Cambridge University Press.
- [3] Holt, R. D. and G. A. Polis (1997): A theoretical framework for intraguild predation, *American Naturalist* 149:745-764.
- [4] Wang, W., G. Mulone, F. Salemi and V. Salone (2001): Permanence and Stability of a Stage-Structured Predator-Prey Model, *Journal of Mathematical Analysis and Applications* 262, 499-